Photonic Crystal Fiber Biosensor for Environmental Pollutants Detection

Rudi Salam
Faculty of Integrated Technologies
Universiti Brunei Darussalam
Bandar Seri Begawan, Brunei
21h8458@ubd.edu.bn

Abdul Mu'iz Maidi
Faculty of Integrated Technologies
Universiti Brunei Darussalam
Bandar Seri Begawan, Brunei
21m5101@ubd.edu.bn

Min Cheng
CQC Standard Testing Technology
(Shanghai) Co., Ltd
Shanghai, China
minchengdl@163.com

Kai Liu
CQC Standard Testing Technology
(Shanghai) Co., Ltd
Shanghai, China
185312597@qq.com

Nianyu Zou
Research Institute of Photonics
Dalian Polytechnic University
Dalian, China
n_y_zou@dlpu.edu.cn

Norazanita Shamsuddin
Faculty of Integrated Technologies
Universiti Brunei Darussalam
Bandar Seri Begawan, Brunei
norazanita.shamsudin@ubd.edu.bn

Feroza Begum
Faculty of Integrated Technologies
Universiti Brunei Darussalam
Bandar Seri Begawan, Brunei
feroza.begum@ubd.edu.bn

***Abstract*—A simple photonic crystal fiber biosensor design for pollutants detection has been numerically studied that depicted high sensitivities over 94% and low confinement losses about 10^{-14} dB/m for sarin, soman, and tabun, at optimum frequency.**

Keywords—Photonic crystal fiber, pollutants, relative sensitivity, confinement loss

I. Introduction

Photonic Crystal Fibers (PCFs) have recently found new applications in sensing, in addition to their common use in optical communication, imaging, and other areas [1]–[3]. PCFs have been utilized to measure and detect various parameters, including temperature, chemicals, pressure, liquid, gas, and many more [4]–[6]. Recent research has shown that certain pollutants can have long-term effects on human health. For example, Sarin (GB), Soman (GD), and Tabun (GA) are pollutants that can pose serious risks if left unchecked. Sarin is one of the most dangerous gases for humans, which can cause coma and eventually death, disrupt the normal functioning of the nervous system, and inhibit the enzyme cholinesterase. Soman and tabun can cause sweating, blurred vision, headaches, and difficulty breathing [7], [8]. Therefore, there is a need for a dedicated device for sensing and detecting pollutants.

Hossian *et al*. [7] introduced a PCF-based chemical sensor model is a rectangular core PCF sensor is offered for the detection of bane chemicals (Sarin, Soman and Tabun) in THz frequency region, where Zeonex is used as fiber material. The optimum model shows enhanced relative sensitivity of around 91.84% for Sarin, 93.45% for Soman, and 94.4% for Tabun at the frequency of 1.8 THz [7]. Besides, a group of researchers [8] found that relatively enhanced relative sensitivity of 91.2%, 91.7%, and 92.7% for Sarin, Soman, and Tabun, respectively, is achieved by their presented sensor design, which the foremost requirement to provide the best performance by chemical sensor. Despite the intricate designs of these prior PCF sensors [7], [8], the relative sensitivity outcomes, while enhanced, remain within the lower range of sensitivity results for the detection of the mentioned pollutant analytes.

Therefore, a simple and effective PCF sensor that follows the same background material of Zeonex, for the purpose of detecting pollutants is necessary. It has been designed with 1 circular core hole and 13 cladding air holes. To evaluate the performance of the sensor, optical parameters such as effective refractive index, power fraction, relative sensitivity, and confinement loss are examined in the 0.6 to 1.8 THz range. The results show that the proposed sensor has obtained relative sensitivity over 94% and confinement losses less than 10^{-14} dB, at the optimal frequency. These values indicate a high level of accuracy and sensitivity in detecting pollutants.

II. Design

The PCF sensor design consists of 3 primary components: the core, the cladding, and the perfectly matched layer (PML). The core exists a singular core hole for infiltration of the pollutants to be detected, and a total of 13 cladding air holes (12 circular holes around a hexagonal ring hole). Fig. 1 shows the simple proposed sensor design for pollutants sensing.

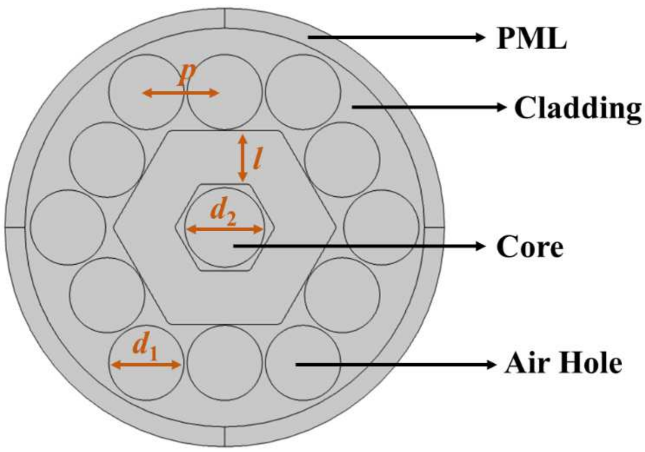

Fig. 1. Propose PCF sensor.

A PML boundary condition is applied to the fiber to prevent light propagating back within the waveguide [9]. The core hole diameter and the cladding air hole diameter is represented as d_1 and d_2, respectively. A hexagonal ring is imposed in the cladding, around the core hole, with thickness denoted as l. The pitch p is the distance between the center of the neighboring cladding air holes. The background material is Zeonex, with refractive index $n = 1.53$ [7], [8].

The design configuration has a pitch spacing p of 600 µm, diameter d_1 is 576 µm, d_2 is 611 µm, and thickness $l = 546$ µm. The PML has been set to 10% of the fiber diameter to ensure effective absorption of light leakage, the overall fiber diameter is 3366 µm.

III. Methodology

The COMSOL Multiphysics version 5.6 is used to simulate and analyze the fiber design in order to evaluate the performance of the aforementioned PCF sensor design. The study's specified operating frequency ranges from 0.6 to 1.8 THz. Sarin ($n = 1.3660$), soman ($n = 1.394$) and tabun ($n = 1.440$) are the refractive indices of the pollutant analytes for sensing [7], [8], that determines the results of power fraction P, relative sensitivity S and confinement loss is L [10]–[15].

$$P = \frac{sample \int Re(E_x H_y - E_y H_x) dxdy}{total \int Re(E_x H_y - E_y H_x) dxdy} \times 100 \quad (1)$$

$$S = \frac{n_r}{Re(n_{\text{eff}})} \times P \quad (2)$$

$$L = \frac{40\pi}{\ln(10)\lambda} Im(n_{\text{eff}}) \times 10^6 \quad (3)$$

where, λ is the operating wavelength, E_x and H_x are the electric and magnetic field in the transverse direction, whilst E_y and H_y are the electric and magnetic field in the longitudinal direction, n_r is the refractive index of the sensed material, $Im(n_{\text{eff}})$ is the imaginary part of the effective mode index.

IV. Results and Discussion

The effectiveness of the proposed pollutant sensor's detection capabilities can be determined by evaluating key optical properties such as effective refractive index, power fraction, relative sensitivity, and confinement loss. Fig. 2 shows the relationship between the effective refractive indices of sarin, soman, and tabun and the operating frequency, with the effective refractive indices of these pollutants increasing in the terahertz frequency range from 0.6 to 1.8 THz. This trend concurs due to its refractive indices of each analyte and the combination with the background material. Tabun has higher effective refractive index due to its high respective refractive index n, followed by soman, then sarin.

Fig. 3 displays the power fraction data for sarin, soman, and tabun as a function in terahertz frequency. The power fractions of these pollutants are observed to gradually increase significantly at lower frequency before gradually decreasing with increasing frequency.

Relative sensitivities of sarin, soman, and tabun against operating frequency are demonstrated in Fig. 4. As identified from the figure, relative sensitivities of the test analytes decrease with respect to operating frequency. Due to the relation to the effective refractive index and power fraction, tabun has a high sensitivity followed by soman, then sarin. At operating frequency $f = 0.8$ THz, the relative sensitivity of sarin is 94.01%, soman is 95.38%, and tabun is 97.10%.

Fig. 5. presents the confinement loss data for the pollutant analytes with respect to frequency. As the frequency increases, light signal becomes more confined in the core of the fiber, which is reflected in the confinement loss values shown in the graph; the confinement loss for all analytes decreases with increasing frequency. The confinement loss values for sarin, soman, and tabun are 1.28×10^{-10} dB/m, 9.41×10^{-12} dB/m, and 7.87×10^{-14} dB/m, respectively.

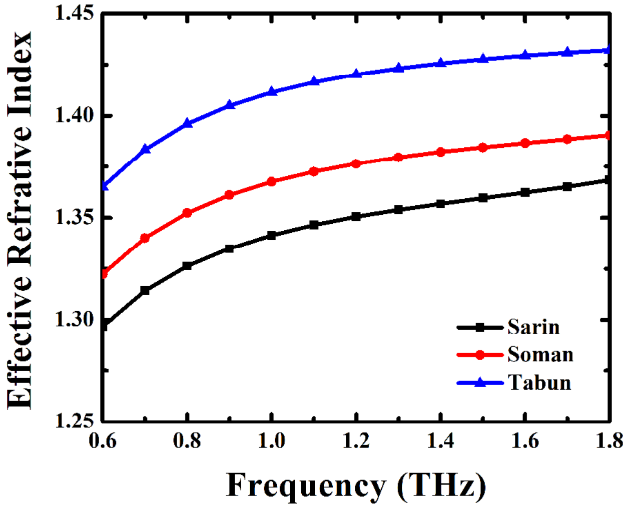

Fig. 2. Results of the effective refractive index of the proposed PCF for sarin, soman, and tabun.

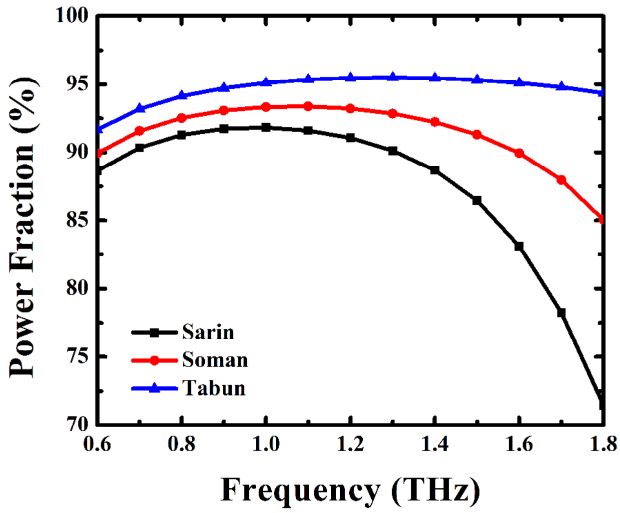

Fig. 3. Results of the power fraction of the proposed PCF for sarin, soman, and tabun.

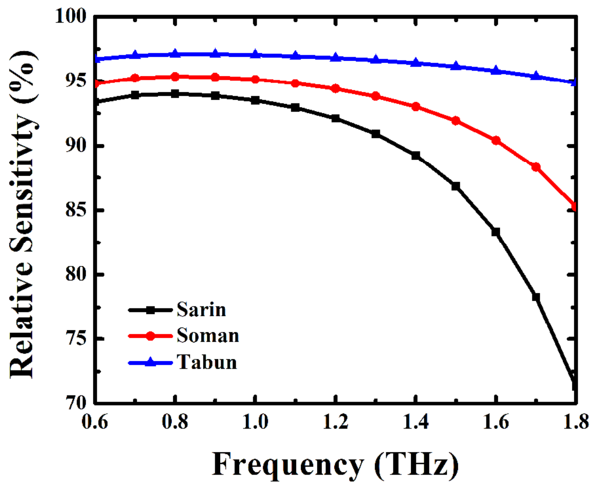

Fig. 4. Results of the relative sensitivity of the proposed PCF for sarin, soman, and tabun.

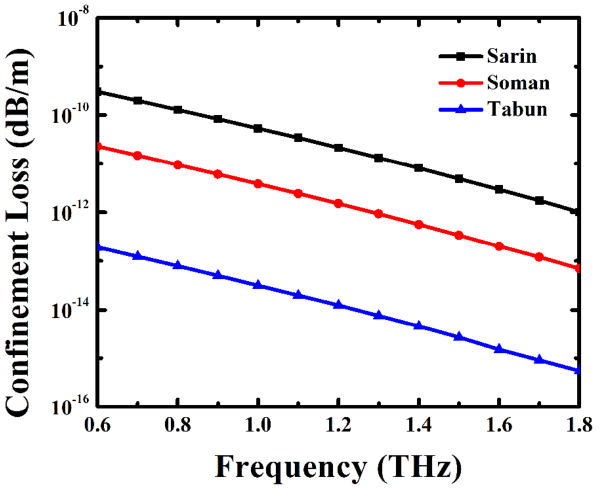

Fig. 5. Results of the confinement loss of the proposed PCF for sarin, soman, and tabun.

Table 1 provides a comparison of the results obtained from the proposed PCF sensor design with the prior designs. It demonstrates that the proposed PCF design yields superior outcomes in terms of relative sensitivity and confinement loss. Relative sensitivities, which reflect the sensing capabilities of fiber design, are significantly improved. Moreover, the PCF design exhibits lower confinement loss that indicates a higher degree of light confinement within the structure. These findings, thus, highlight the efficacy and enhanced performance, making it a more promising advancement in the field of pollution sensing.

TABLE I. COMPARISON OF PROPOSED PCF SENSRO RESULTS AGAINST PREVIOUS PCFS

Reference	Relative Sensitivity (%)			Confinement Loss (dB/m)		
	Sarin	***Soman***	***Tabun***	***Sarin***	***Soman***	***Tabun***
Ref. [7]	91.84	93.45	94.40	-	-	-
Ref. [8]	91.2	91.7	92.7	-	-	-
Proposed PCF	94.01	95.38	97.10	$\sim 10^{-10}$	$\sim 10^{-12}$	$\sim 10^{-14}$

V. CONCLUSION

A simple structure of Zeonex-based photonic crystal fiber biosensor for the detection pollutants of sarin, soman, and tabun has been proposed, operating in the 0.6 to 1.8 THz range. At the optimal frequency of 0.8 THz, the sensor design depicts high relative sensitivities of 94.01% for sarin, 95.38% for soman, 97.10% for tabun, and 1.28×10^{-10} dB/m for sarin, 9.41×10^{-12} dB/m for soman, and 7.87×10^{-14} dB/m for tabun for the confinement loss. Accordingly, these outcomes determine the capabilities of detecting these selected test analytes in actual sensing applications.

ACKNOWLEDGMENT

Sincere gratitude to Min Cheng and Kai Liu from CQC Standard Testing Technology (Shanghai) Co., Ltd and Nianyu Zou from Research Institute of Photonics at Dalian Polytechnic University for their invaluable contribution to the conference. Their participation in the conference has been instrumental in its success, and their contributions are deeply appreciated.

REFERENCES

[1] M. Ahasan Habib, M. Shamim Anower, and M. Nazmul Islam, “Terahertz Sensing Based on Photonic Crystal Fibers,” *Terahertz Technol.*, 2022, doi: 10.5772/intechopen.101732.

[2] F. Begum *et al.*, “Flattened chromatic dispersion in square photonic crystal fibers with low confinement losses,” *Opt. Rev.*, vol. 16, no. 2, pp. 54–58, Mar. 2009, doi: 10.1007/s10043-009-0011-x.

[3] N. H. Hai *et al.*, “A unique approach in ultra-flattened dispersion photonic crystal fibers containing elliptical air-holes,” *Opt. Rev.*, vol. 15, no. 2, pp. 91–96, Mar. 2008, doi: 10.1007/s10043-008-0013-0.

[4] A. Abbaszadeh, S. Makouei, and S. Meshgini, “New hybrid photonic crystal fiber gas sensor with high sensitivity for ammonia gas detection,” *Can. J. Phys.*, vol. 100, no. 2, pp. 129–137, Feb. 2022, doi: 10.1139/cjp-2021-0016.

[5] M. R. Islam *et al.*, “Design of a hexagonal outlined porous cladding with vacant core photonic crystal fibre biosensor for cyanide detection at THz regime,” *IET Optoelectron.*, vol. 16, no. 4, pp. 160–173, Aug. 2022, doi: 10.1049/ote2.12067.

[6] E. K. Akowuah, T. Gorman, H. Ademgil, S. Haxha, G. K. Robinson, and J. V. Oliver, “Numerical Analysis of a Photonic Crystal Fiber for Biosensing Applications,” *IEEE J. Quantum Electron.*, vol. 48, no. 11, pp. 1403–1410, Nov. 2012, doi: 10.1109/JQE.2012.2213803.

[7] M. B. Hossain, E. Podder, A. A.-M. Bulbul, and H. S. Mondal, “Bane chemicals detection through photonic crystal fiber in THz regime,” *Opt. Fiber Technol.*, vol. 54, p. 102102, Jan. 2020, doi: 10.1016/j.yofte.2019.102102.

[8] R. H. Jibon, S. Biswas, S. Biswas, and N. F. I. Nira, “Poisonous chemical detection in the THz regime using PCF: Design and numerical investigation,” *J. Opt.*, vol. 50, no. 4, pp. 671–680, Dec. 2021, doi: 10.1007/s12596-021-00737-4.

[9] A. M. Maidi, M. A. Kalam, and F. Begum, “Photonic Crystal Fiber Sensor for Detecting Sulfuric Acid in Different Concentrations,” *Photonics*, vol. 9, no. 12, p. 958, Dec. 2022, doi: 10.3390/photonics9120958.

[10] A. M. Maidi *et al.*, “Design and Simulation of Photonic Crystal Fiber for Liquid Sensing,” *Photonics*, vol. 8, no. 1, p. 16, Jan. 2021, doi: 10.3390/photonics8010016.

[11] I. K. Yakasai, P. E. Abas, H. Suhaimi, and F. Begum, “Low loss and highly birefringent photonic crystal fibre for terahertz applications,” *Optik (Stuttg).*, vol. 206, p. 164321, Mar. 2020, doi: 10.1016/j.ijleo.2020.164321.

[12] M. E. Rahaman, R. H. Jibon, H. S. Mondal, M. B. Hossain, A. A.-M. Bulbul, and R. Saha, “Design and optimization of a PCF-based chemical sensor in THz regime,” *Sens. Bio-Sensing Res.*, vol. 32, p. 100422, Jun. 2021, doi: 10.1016/j.sbsr.2021.100422.

[13] M. M. Hasan, T. Pandey, and M. A. Habib, “Highly sensitive hollow-core fiber for spectroscopic sensing applications,” *Sens. Bio-Sensing Res.*, vol. 34, p. 100456, Dec. 2021, doi: 10.1016/j.sbsr.2021.100456.

[14] E. Podder, R. H. Jibon, M. B. Hossain, A. Al-Mamun Bulbul, S. Biswas, and M. A. Kabir, “Alcohol Sensing through Photonic Crystal Fiber at Different Temperature,” *Opt. Photonics J.*, vol. 08, no. 10, pp. 309–316, 2018, doi: 10.4236/opj.2018.810026.

[15] A. M. Maidi, N. Shamsuddin, W.-R. Wong, S. Kaijage, and F. Begum, “Characteristics of Ultrasensitive Hexagonal-Cored Photonic Crystal Fiber for Hazardous Chemical Sensing,” *Photonics*, vol. 9, no. 1, p. 38, Jan. 2022, doi: 10.3390/photonics9010038.